J Fluoresc (2015) 25:861–870
DOI 10.1007/s10895-015-1566-5

ORIGINAL PAPER

Determination of Glucose and Cholesterol Using a Novel Optimized Luminol- CuO Nanoparticles-H_2O_2 Chemiluminescence Method by Box–Behnken Design

Mohammad Javad Chaichi[1] · **Mahjoobeh Ehsani**[1]

Received: 19 July 2014 / Accepted: 9 April 2015 / Published online: 26 May 2015

Abstract In this study, a simple, rapid and sensitive luminol-CuO nanoparticles-H_2O_2 chemiluminescence (CL) method has been proposed for determination of glucose and cholesterol in plasma. Response surface methodology (RSM) based on Box–Behnken design (BBD) was used to optimize the most important operating variables (solution pH effect and the CL reagents concentration) of luminol CL system. In optimum conditions, it was found that CuO nanoparticles (NPs) could enhance the CL intensity and the method sensitivity towards evaluation of trace amount of glucose and cholesterol. Under the optimal conditions, there is a good linear relationship between the luminol-CuO NPs - H_2O_2 relative CL intensity and the concentration over the range of 1.2×10^{-6}–1.0×10^{-3} M (R^2=0.9991) for glucose and 2.5×10^{-5}–CuO NPs7.17×10^{-3} M (R^2=0.9968) for cholesterol and with a 3σ detection limit of 7.1×10^{-7} and 6.4×10^{-6} M, respectively. The relative standard deviations (RSD)<3.3% were obtained.

Keywords Luminol chemiluminescence · Box-Behnken design · Glucose · Cholesterol · CuO nanoparticles

Introduction

Chemiluminescence (CL), which is the phenomenon observed when the vibronically excited product of an exoergic chemical reaction relaxes to its ground state with emission of photons, can be defined in simplistic terms: chemical reactions that emit light [1, 2]. CL detection has many advantages, such as high sensitivity, wide calibration range, relatively simple and inexpensive instrument, rapidity in signal detection (normally 0.1–10 s) and suitable for automation [3, 4]. But the CL emission generated during oxidation of organic molecules is of relatively low intensity due to low quantum yield [5–7]. Since the CL phenomenon of luminol was first reported by Albrecht in 1928 [8], investigation of effective catalysts for such CL reactions has been carried out, including metal ions, metal complex, and enzymes. The catalyzed luminol chemiluminescent reaction has received, a great amount of attention because of its high sensitivity and low background signal which make the reaction as an attractive analytical chemistry tool in various fields, such as biotechnology, food analysis, environmental analysis, pharmaceutical analysis and clinical assay [9–11]. Metal nanoparticles (NPs) because of their unique redox catalytic, optical, electronic, chemical and mechanical properties have gained increasing attention in recent years [12, 13]. Also, nanoparticles as a novel alternative to catalyze redox CL reactions, under proper conditions, can provide amplified CL emission for the ultrasensitive detection of biological species [12–15]. Copper oxide (CuO) is a p-type semiconducting compound with a monoclinic structure and a narrow (1.2–1.8 ev) band gap. It is used in various technological applications such as high critical temperature superconductors, gas sensors, in photoconductive, photocatalytic or photovoltaic applications, and so on. Furthermore, CuO NPs possess an almost unchanged catalytic activity over a wide range of pH and temperatures and exhibited significant peroxidase-like activity [16–18]. Quantitative determination of glucose and cholesterol is very important in biochemistry, clinical chemistry, food processing and fermentation [19–24]. The clinical conditions of diabetes mellitus are well known and understood, yet remain a growing concern as the prevalence of the disease increases worldwide at an alarming rate [19–22]. Cholesterol is the main sterol component in body

✉ Mohammad Javad Chaichi
jchaichi@yahoo.com

[1] Faculty of Chemistry, University of Mazandaran, Babolsar, IR, Iran

tissues occurring mainly in the brain and spinal cord. This important biomolecule maintains membrane fluidity and acts as a precursor in the production of Vitamin D and hormones [23–26]. Increased plasma levels are associated with atherosclerosis, nephritis, diabetes mellitus and obstruction jaundice [23–26]. To date, the most common glucose and cholesterol determination methods are based on the electrochemical or spectrophotometrical detection of hydrogen peroxide liberated in enzymatic reaction. Enzymatic method yields maximum specificity for glucose and cholesterol estimation [19, 24]. However, these both methods are subject to several interferences including reducing substances such as bilirubin, ascorbic acid, uric acid, and drug metabolites [27, 28]. Other disadvantage of these methods is lack of sensitivity. These problems seriously limit their application in complex matrix such as physiological samples containing low content of glucose, cholesterol and high amounts of interferences. Glucose in presence of oxygen react with glucose oxidase and produce D-gluconic acid and hydrogen peroxide (H_2O_2) [29]. Cholesterol esters in serum are hydrolyzed by cholesterol esterase (CHE). The free cholesterol produced is oxidized by cholesterol oxidase (CHO) to cholest-4-en-3-one with the simultaneous production of H_2O_2, which oxidatively couples with 4-aminoantipyrine and phenol in the presence of peroxidase to yield a chromophore can be measured spectrophotometrically at 540/600 nm as an increase in absorbance [30]. The coupling of the nanocatalyzed luminol CL reaction with enzymatic reactions can significantly increase both the sensitivity and selectivity of the glucose determination methods, thus providing the basis for development of a number of sensitive methods of analysis [12]. Similar to all analytical methods, the factors involving CL measurements are not commonly independent. Multivariate experimental design techniques, which allow the simultaneous optimization of several variables, are faster to implement and more cost-effective than traditional univariate (one at a time) approaches [31]. In this study we proposed a simple and fast CL method for the determination of glucose and cholesterol in plasma in the presence of CuO NPs as an effective catalyst. The optimization of effective factors on the CL intensity has been carried out by using Box-Behnken design [32].

Experimental

Reagents and Materials

All the solutions were prepared using reagent grade chemicals and deionized–distilled water was used throughout. Cupric acetate monohydrate, sodium hydroxide, glucose. cholesterol and 30% (v/v) H_2O_2 were supplied from Merck chemical company. A 0.01 M stock solution of luminol (Sigma) was prepared by dissolving 0.1772 g in 0.01 M sodium hydroxide solutions. Working solution of luminol was prepared by diluting the stock solution with 0.1 M phosphate buffer solution to adjust the pH in the various ranges. A stock solution of H_2O_2 was prepared by appropriate dilution of 30% solution with water. Glucose oxidase (GOx), cholesterol oxidase (CHO) and cholesterol esterase (CHE) were purchased from Zist-chimi. Stock standard solutions 10^{-2} M of glucose and cholesterol (Amresco, Solon, Ohio) were prepared and the standard solutions were prepared by proper dilution of the stock. The phosphate buffer was prepared by mixing the appropriate amount of Na_2HPO_4 (0.1 M) and NaH_2PO_4 (0.1 M) in water.

Synthesis of Cupric Oxide Nanoparticles

The cupric oxide nanoparticles were prepared via quick-precipitation method [33]. Briefly, 150 mL of 0.02 M copper acetate aqueous solution was mixed with 0.5 ml glacial acetic acid in a round-bottomed flask equipped with a refluxing device. The solution was heated up to 80 °C with vigorous stirring. Then10mL of 0.04 g mL^{-1} NaOH aqueous solution was (rapidly added into) gradually dropped into the above boiling solution under magnetic stirring until the mixture's pH reached the value of 6.0–7.5, where a great quantity of black precipitate was simultaneously produced. The precipitate was centrifuged, washed several times with absolute ethanol and deionizer water, and dried in air at room temperature. Then, powders were annealed for 1 h at temperature of 400 °C, to obtain the highly crystalline CuO NPs. The morphology and size distribution of the synthesized CuO nanoparticles were characterized by using Fourier Transform Infrared Spectroscopy (FT-IR) and X-ray diffraction (XRD). The as-prepared CuO nanoparticles, even without any surface modification, can well disperse in distilled water to form a transparent brown solution. The study shown that the UV–Vis absorption spectrum of the solution remains unchanged even after 6 months, which plays an important role in our later experiments in chemiluminescence system (Fig. 1).

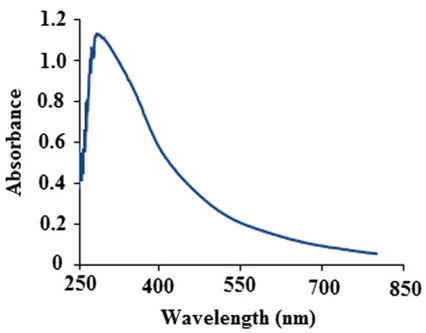

Fig. 1 UV–vis spectrum of colloidal CuO nanoparticles

Table 1 The chosen levels and codes of variables for Box- Behnken design

Variable	Symbol	Low (−1)	Middle(0)	High(+1)
Luminol concentration(M)	X_1	5×10^{-5}	10^{-4}	5×10^{-4}
pH	X_2	6	7	8
H_2O_2concentration (M)	X_3	10^{-4}	5×10^{-4}	10^{-3}

Apparatus and Software

The chemiluminescence (CL) signal was monitored using a Sirius Single Tube Luminometer (Berthold, Germany). CL intensity was recorded as a function of time and the time resolution of the apparatus was 1 s. Absorption spectra were recorded using UV–Vis spectrophotometer (Cecil, CE5501). An x-ray diffraction (XRD) pattern was performed using PHILIPS Xpert pro diffractometer with Cu Kα radiation (λ 1.54 A°). Scanning electron microscopic (SEM) images were observed under CAMScan-MV2300 instrument (England). A model 710 Metrohm pH meter was used to carry out the pH measurements. Also, 15 experimental runs (formulation combinations) for optimization of factor levels, was generated and analyzed using Minitab 16 software.

Experimental Design and Statistical Analysis

Based on the results of single-factor experiments a 3-level, 3-factor Box-Behnken design requiring 15 experiments was performed for optimization of chemiluminescence conditions such as pH and concentrations of luminol and hydrogen peroxide to acquire the maximum intensity. Table 1 represents the levels of each factor. The experimental data in terms of CL intensity are recorded in Table 2. Experimental design and statistical analysis of the results were performed by Minitab statistical Software. All experiments were repeated three times.

General Procedure for CL Detection

The chemiluminescence measurements were carried out by a Siriustube luminometer (Berthold detection system, Germany) with a photomultiplier (PMT) tube detector. Solution (I) was made with mixing 200 μL of luminol (various pH in 0.1 M phosphate buffer) at particular concentrations, 30 μL of colloidal CuO NPs (0.2 mgL^{-1}). Solution (II) was made by mixing 250 μL of glucose or cholesterol (various concentration in 0.1 M phosphate buffer) and 250 μL of glucose oxidase 250UdL^{-1} or (cholesterol esterase and cholesterol oxidase mixture solution) in 0.1 M phosphate buffer (10^{-3} M) in a dark glass cell. After 20 min solution (I) was transferred into glass cell and then 200 μL of solution (II) was injected in the glass cell using polypropene syringes, chemiluminescence spectrum was recorded soon after mixing the solutions.

Result and discussion

Enhancement of Luminol CL

The effects of cupric oxide nanoparticles-H_2O_2 chemiluminescent system were investigated. As shown in

Table 2 Design matrix and corresponding response variable (CL intensity) for the Box-Behnken design

Factors				Experimental CL intensity	Estimate CL intensity	Residual	SE
Run	[Luminol] X_1	pH X_2	[H_2O_2] X_3				
1	0	0	0	332.00	322.437	9.5633	6.49816
2	0	−1	1	298.00	301.857	−3.8575	9.74725
3	−1	−1	0	5.84	−4.988	10.8275	9.74725
4	1	0	1	680.00	675.310	4.6900	9.74725
5	0	1	−1	405.41	401.552	3.8575	9.74725
6	1	0	−1	433.30	426.330	6.9700	9.74725
7	−1	0	−1	14.50	19.190	−4.6900	9.74725
8	1	1	0	740.00	750.828	−10.8275	9.74725
9	−1	0	1	308.00	314.970	−6.9700	9.74725
10	0	1	1	675.23	669.093	6.1375	9.74725
11	−1	1	0	340.00	339.167	−0.8325	9.74725
12	0	−1	−1	18.50	24.637	−6.1375	9.74725
13	1	−1	0	350.00	350.833	−0.8325	9.74725
14	0	0	0	315.00	322.437	−7.4367	6.49816
15	0	0	0	320.31	322.437	−2.1267	6.49816

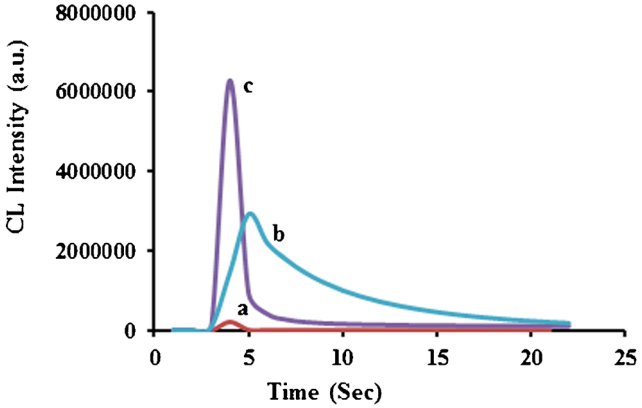

Fig. 2 Time course of the kinetic profiles of the luminol–H_2O_2 CL reaction: **a** without CuO nanoparticles, **b** with the nanoparticles at pH 10, **c** with the nanoparticles at pH 7

Fig. 2, the kinetic curve shows that the oxidation of luminol by H_2O_2 generates weak CL in alkaline media. In presence of cupric oxide nanoparticles, the CL signal intensity could be greatly enhanced up to about, 28 folds. Because our main goal was study and using the proposed chemiluminescence method in biological condition (pH=7), we considered the catalytic effect of CuO nanoparticles on the luminol- H_2O_2 system at pH 7. The results show that CuO nanoparticles enhance the luminol- H_2O_2 chemiluminescence intensity up to about, 13 folds (Fig. 2). Fig. 2 indicates the chemiluminescence emission intensity as a function of time for the luminol–H_2O_2 CL system: (a) without CuO nanoparticles, (b) with CuO nanoparticles at pH 10 and (c) with CuO nanoparticles at pH 7.

Characterization of CuO Nanoparticles

The compositions of precipitated fine particles were characterized by XRD and SEM for structural determination and estimation of crystallite size. The XRD pattern of the synthesized CuO nanoparticles was shown in Fig. 3. The

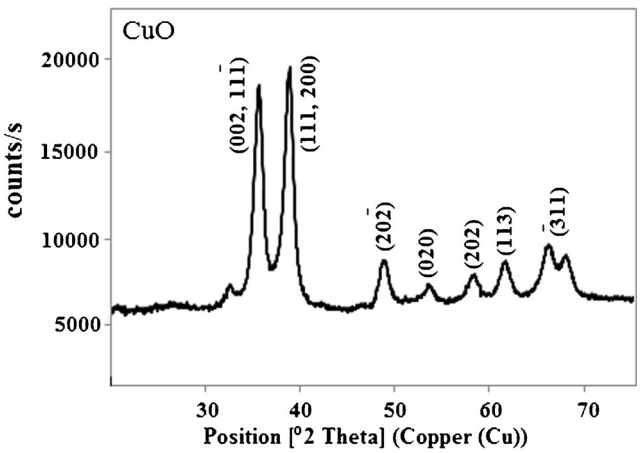

Fig. 3 XRD pattern of CuO nanoparticles

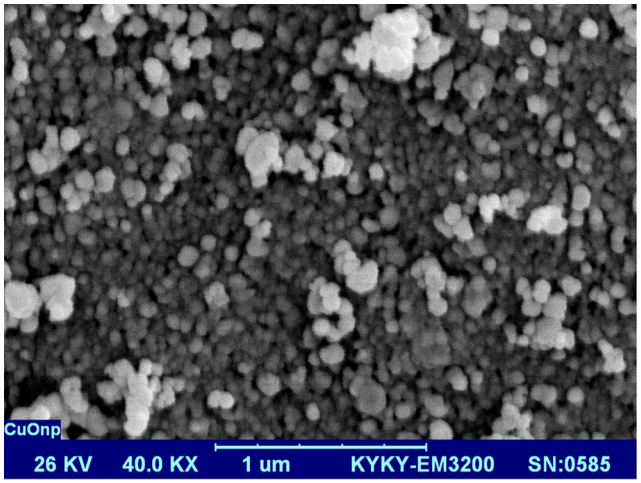

Fig. 4 SEM image of prepared CuO nanoparticles

structural peaks of CuO nanoparticles are observed. XRD patterns (Fig. 3) of the products obtained are identical to the single-phase CuO and the diffraction data were in good agreement with JCPDS card of CuO (JCPDS 80–1268). Also no peaks of impurity were observed in the XRD patterns. The broad peaks indicate the small size of the products. Actually, the average size (D) of the CuO nanoparticles can be calculated according to Scherrer's equation [34]:

$$D = k(\lambda/\beta\cos\theta) \quad (1)$$

where k is a constant(shape factor,about0.89), λ is the X-ray wavelength (0.15418 nm), β is the full-width at half-maximum (FWHM) value of the strongest reflection of the (111) peak, and θ is the diffraction angle. Based on the Scherrer's equation, the average size of CuO nanoparticles was estimated to be 19.6 approximately. The structures of the samples were examined by a SEM image. Figure 4 shows the SEM image of prepared CuO NPs. It is observed that the CuO NPs are synthesized in spherical

Table 3 Test of significance for regression coefficients

Coefficient	Coefficient Value	Standard error	Significance level (p)
β_0	322.437	6.468	0.000
β_1	191.870	3.961	0.000
β_2	186.038	3.961	0.000
β_3	136.190	3.961	0.000
β_{11}	23.094	5.830	0.011
β_{22}	13.429	5.830	0.070
β_{33}	13.419	5.830	0.071
β_{12}	13.960	5.602	0.056
β_{13}	−11.700	5.602	0.092
β_{23}	−2.420	5.602	0.685

Table 4 Analysis of variance table (ANOVA) of BBD design for CL intensity

Source	DF	Sum of square	Mean square	F-ratio	*p*- value Prob>F
Regression	9	724035	80437	*635.06	0.000
Residual error	5	633	126		
Lack-of-Fit (LOF)	3	482	161	2.12	0.336
Pure error	2	151	73		
Total	14	724638			

R^2 =0.9991, R^2 (adj)=0.9976, $F_{0.01}$ (9, 5)=10.15, $F_{0.01}$(3, 2)=99.17; *Significant at 1% level

shape and uniform structure, relatively. However, some aggregated particles can be observed in the images because of aggregation during separation and drying. For sample the size of the particles observed in the SEM picture is within the range of 24.2–33.2 nm.

Optimization of Experimental Conditions

The optimum conditions for maximizing the CL emission intensity were determined by means of a Box–Behnken experimental design combining with response surface modeling (RSM) and quadratic programming. RSM is a statistical and graphical technique for developing, improving and optimizing process which can overcome the following disadvantages: the classical one-factor-one-time design method in a time-consuming process; unrealistic number of experiments and difficulties in determination of optimal conditions. Box-Behnken design is an especially efficient response surface method for obtaining mathematical models [35]. The number of experiments (N) required for BBD development is defined as:

$$N = 2K(K-1) + C_0 \quad (2)$$

Where K is the number of factors and C_0 is the number of central points [36]. In this study, the most important factors that found from preliminary experiments are H_2O_2 concentration, luminol concentration and pH. These three significant factors are used to determine the optimal conditions and examined in more detail using response surface designs. The Box–Behnken design has 15 experimental runs with three runs at the center point (Table 2). The experimental data was fitted into a second-order equation and the quadratic equation model is as the following:

$$Y = \beta_0 + \sum_{i=1}^{k} \beta_i x_i + \sum_{i=1}^{k} \beta_{ii} x_i^2 + \sum_{i=1}^{k} \sum_{i=1}^{k} \beta_i x_i x_j + \varepsilon \quad (3)$$

where Y is the output or the CL emission intensity of luminol- CuO NPs- H_2O_2 system (dependent variable), k is the number of the patterns, i and j are the index numbers for pattern, β_0 is the free or offset term called intercept term, x_1, x_2,. . ., x_k are the coded independent variables, β_i is the first-order (linear) main effect, β_{ii} is the quadratic (squared) effect, β_{ij} is the interaction effect, and ε is the random error or allows for discrepancies or uncertainties between predicted and measured values [37].

In order to evaluate the effects of luminol concentration (x_1), reaction pH (x_2) and H_2O_2 concentration (x_3) on chemiluminescence intensity, a 3-factor and 3-level Box-Behnken design with three center point and response surface methodology were applied to investigate the effects of factors, the optimum levels of these variables and their relationships. Table 1 shows the levels of the independent factors and experimental designs as coded (0, 1, and −1)

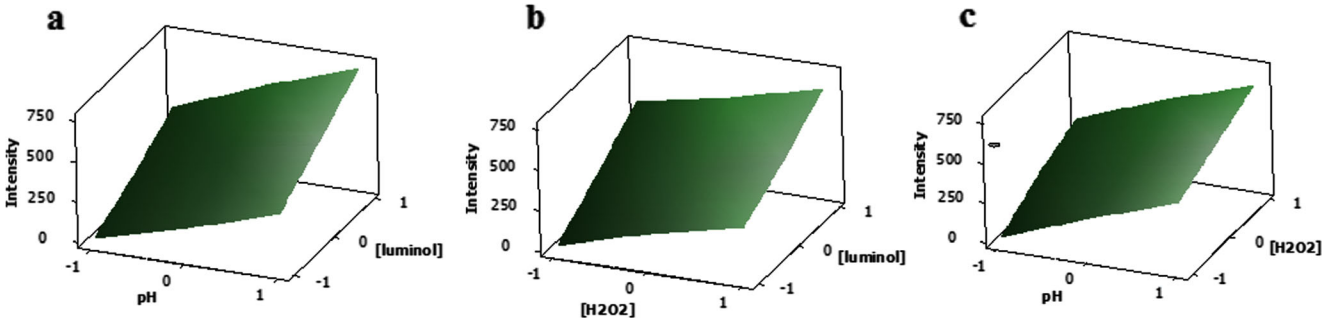

Fig. 5 Diagrams **a**, **b** and **c** show the response surface plots for the three independent effective variables and CL intensity of the luminol-CuO NPs- H_2O_2 system as a dependent variable

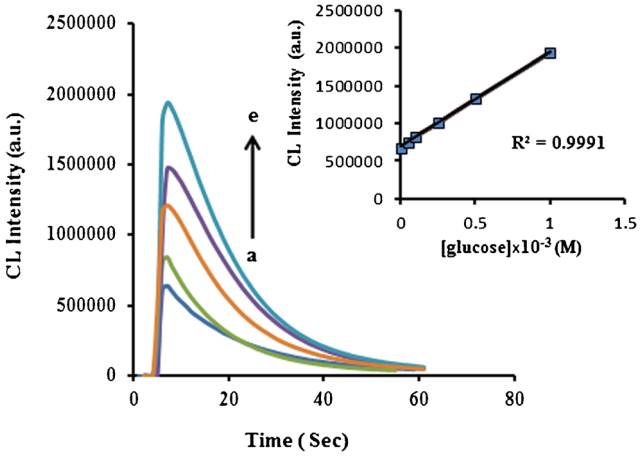

Fig. 6 Chemiluminescence emission intensity as a function of time for the luminol-CuO NPs- H_2O_2 system with constant concentration of luminol (1.0×10^{-4} M), buffer phosphat (0.1 M), CuO NPs (0.2 mgL^{-1}), GOx enzyme ($250UdL^{-1}$), and varying concentrations of glucose: **a** 1.2×10^{-6}, **b** 5.0×10^{-6}, **c** 5.0×10^{-5}, **d** 5.0×10^{-4}, **e** 1×10^{-3} M. Inset: The correlation diagram for thechemiluminescence emission with glucose concentrations

and uncoded (actual value). A total of 15 experiments were required for the optimization process. The design matrix and the responses are illustrated in Table 2. The experiments were run in random manner to overcome the effects of uncontrolled factors. The Minitab software was used to analyze the experimental results. By apply regression analysis a quadratic polynomial equation was established to explain the relationship between the CL intensity and independent variables as follows:

$$Y = 323.103 + 191.870X_1 + 186.038X_2 + 136.190X_3 + 22.761X_1{}^2 - 13.096X_2{}^2 - 13.086X_3{}^2 - 13.096X_1X_2 - 11.700X_1X_3 - 2.420\,X_2X_3 \quad (4)$$

Where Y is the CL emission intensity of luminol- CuO NPs- H_2O_2 system. The analysis of variance (ANOVA) was done to test the significance of the model as given in Table 3. As shown in Table 3, this quadratic polynomial model was highly significant and sufficient to represent the actual relationship between the response and the three parameters with a very low p-value (0.0001) while the lack of the fitted value of the model was 0.336 ($P>0.01$, not significant) (Table 4).

The coefficient of determination (R^2) value was 0.9991. This result revealed that model could explain 99.91% of the variability in the response. Therefore, this model was adequate to predict the CL intensity results within the range of the variables employed. Both of the values indicated that the regression model was valid for the present study. In this study, in order to achieve a better understanding of the effects of the independent variables and their interactions on CL emission intensity, 3D response surface plots for the measured responses were generated based on the model equation (Eq. 4). As the regression model has three independent variables, one variable was kept at constant at the center level for each plot, thus, a total three response 3D plots were formed for responses. Figure 5 shows the 3D response surfaces as the functions of two variables at the center level of other variables. By solving the Eq. 3 and also by analyzing three-dimensional response surface (Fig. 5), the following optimum values of these significant factors were obtained: a 5.0×10^{-4} M luminol concentration, 1.0×10^{-3} M H_2O_2 concentration, a 0.2 mg/L

CuO NPs concentration and a 8 pH value. In the optimum condition the highest CL emission intensity was achieved and corresponding to Fig. 5, all of the independent variables have the most positive effect on the CL intensity at their highest levels.

Application of the Proposed Method for Determination of Glucose and Cholesterol in Human Plasma Sample

In order to examine the applicability of the proposed method, we measured the analytes concentration in the real samples. Plasma

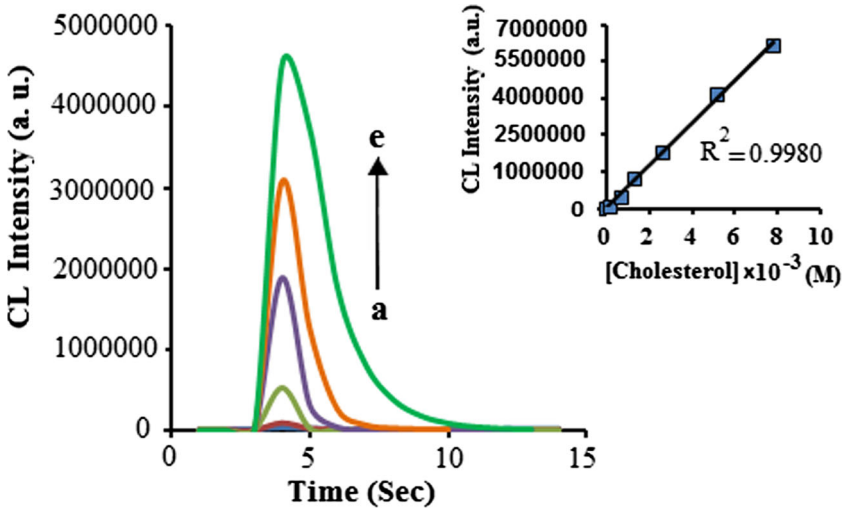

Fig. 7 Chemiluminescence emission intensity as a function of time for the luminol-CuO NPs- H_2O_2 system with constant concentration of luminol (1.0×10^{-4} M), buffer phosphat (0.1 M), CuO NPs (0.2 mgL^{-1}), CHE and CHO enzymes mixture ($250UdL^{-1}$), and varying concentrations of cholestrol: **a** 2.5×10^{-5}, **b** 1.3×10^{-4}, **c** 6.5×10^{-4}, **d** 1.3×10^{-3}, **e** 7.7×10^{-3} M. Inset: The correlation diagram for the chemiluminescence emission with cholestrol concentrations

Table 5 Analytical results of glucose and cholesterol in human serum and recovery test

Sample	Proposed method	Spectrophotometricmethod	Concentration of glucose added ($mgdL^{-1}$)	Concentration of glucose founda ($mgdL^{-1}$)	Reconery(%)	RSD (n=5,%)
Glucose						
Serum 1	94.3±3.5	96.0	10	9.62	96.2	2.8
Serum 2	115.4±2.6	118.0	20	20.44	102.2	2.2
Serum 3	209±1.9	207.0	50	49.0	98.0	3.0
Cholesterol						
Serum 1	116.4	118	10	11.2	112.0	1.5
Serum 2	254.6	250	20	18.9	94.5	3.2
Serum 3	358.0	365	50	52.0	104.0	2.4

samples from different persons were supplied by the diagnostic laboratories (Ghaemshahr and Babolsar, Iran). Plasmas samples were analyzed with photometric kits (Pars Azmoon, Iran) in the laboratories. To examine the reliability of the method certain amounts of standard solution (glucose or cholesterol) was added to the sample solutions and analyzed according to the proposed method. The results show a good and acceptable linear relationship between the luminol-CuO NPs - H_2O_2 relative CL intensity and the concentration in the range of 1.2×10^{-6}–1.0×10^{-3} M (R^2=0.9991) for glucose and 2.5×10^{-5}–7.17×10^{-3} M (R^2= 0.9968) for cholesterol with a low detection limit of 7.1×10^{-7} and 6.4×10^{-6} M, respectively. Chemiluminescence emission intensity as a function of time for the proposed CL system with varying concentrations of glucose and cholesterol and the obtained calibration curves are shown in Figs. 6 and 7. Recovery of each measurement was calculated by comparing the results obtained before and after adding of standard solution and for these experiments the relative standard deviations (RSD)<3.3% were obtained. The results have been listed in Table 5. As compared with other methods reported in the literatures for determination of glucose and cholesterol, the luminol- cupric oxide nanoparticles- H_2O_2- chemiluminescence system exhibit good linear range and low detection limit. The comparative results are shown in Tables 6 and 7.

Interference Study

Glucose and cholesterol are two important components in biological and food samples. Some components of those samples that possibly interfered with glucose and cholesterol determination were tested. In order to study (consideration) of selectivity of the proposed analytical method glucose or cholesterol solution (10^{-5} M) was placed in the reaction cell and increasing amounts of different compounds were added into the solution. A material was considered not to interfere if it caused a relative error <5% during the measurement of 10^{-5} M analyte solution. It was found that the tolerable molar concentration ratios of foreign species to glucose were: 500 for lactose, fructose, bilirubin, tryptophane, Zn^{2+}, SO_4^{2-}, 200 for Fe^{2+}, thiourea, phenylalanine, 100 for sucrose, urea, Ca^{2+}, Mg^{2+}, Cl^-, NO_3^- and to cholesterol were1000 for glycine, Zn^{2+}, 500 for vitamin C, vitamin B_6, urea, tryptophane,

Table 6 Comparison of the linear ranges and detection limits for glucose afforded by the proposed method and other reported methods

Method	Linear range(M)	LOD (M)	Ref.
Biosensor based on rhodamine derivative CL-system	7.72×10^{-6}–2.54×10^{-6}	8.0×10^{-7}	[42]
Immobilized GOX/CNT[a]/Gold NPs in nafion film- TCPO[b]-CL system	2.25×10^{-6}–1.75×10^{-4}	1.0×10^{-6}	[43]
Photopolymerized fluorescence sensor	2.78×10^{-4}–5.56×10^{-6}	0.89×10^{-5}	[44]
Cyclic-voltammetric - gold electrode	1.2×10^{-6}–6.25×10^{-3}	5.0×10^{-7}	[45]
Photoluminescent spectroscopy- CdTe/CdS quantum dots	1.8×10^{-6}–1×10^{-6}	1.8×10^{-6}	[46]
Chemiluminescence - gold NPs	1.0×10^{-5}–1.0×10^{-3}	5×10^{-6}	[47]
Colorimetric bioassay -gold glyconanoparticle	2.77×10^{-3}–2.12×10^{-2}	2.01×10^{-3}	[48]
Amperometric on a polycarbonate microfluidic chip	5.0×10^{-6}–2.0×10^{-3}	4.1×10^{-6}	[49]
Chemiluminescence - CuO NPs	1.2×10^{-6}–1.0×10^{-3}	7.1×10^{-7}	This work

[a] Carbon nano tubes

[b] Bis(2,4,6-trichlorophenyl) oxalate

Table 7 Comparison of the linear ranges and detection limits for cholesterol afforded by the proposed method and other reported methods

Method	Linear range(M)	LOD (M)	Ref.
Electrochemical bienzyme membrane sensor	9.0×10^{-5}–5.5×10^{-2}	$50.\times10^{-6}$	[41]
Cyclic Voltammetry- MWCNTs[a] -MnO_2 Nanoparticles	1.0×10^{-9}–1.0×10^{-7}	0.3×10^{-9}	[50]
Amperometry- Pt-Incorporated Fullerene-like ZnO Nanospheres	2.78×10^{-3}–1.22×10^{-2}	0.5×10^{-3}	[51]
Electrochemical multienzymatic biosensor	0.04×10^{-3}–0.27×10^{-3}		[52]
HPLC–UV [b]	9.25×10^{-6}–9.25×10^{-4}		[53]
Electropolymerized Enzyme Immobilization-Carbon Nanotube Electrode	2.58×10^{-3}–1.55×10^{-2}		[54]
Luminol electrogenerated chemiluminescence-Gold nanoparticles	3.3×10^{-5}–1.0×10^{-3}	1.1×10^{-6}	[55]
Chemiluminescence - CuO nanoparticle	2.5×10^{-5}–7.17×10^{-3}	6.4×10^{-6}	This work

[a] Multi-walled carbon nano tubes

[b] High performance liquid chromatography- ultraviolet visible spectroscopy

billirubine, 200 for Ca^{2+}, 100 for Cu^{2+} and 20 for Fe^{2+}. As it can be seen, the selectivity of the method is high.

CL Mechanism

One of the most remarkable features of metal NPs is their ability to catalyze various redox reactions taking advantage of their unique chemical and electrochemical properties. The catalytic activity of metal NPs of the on the gas-phase and liquid-phase redox CL reactions has been established and has become an expanding field of research [12, 38]. The major CL-generating mechanism for luminol oxidation in aqueous solution has been has been studied and reported previously [39, 40]. We have discussed already, in the introduction section, about enzymatic reaction of glucose and cholesterol. The produced hydrogen peroxide in the result of these selective reactions can be detected in very sensitive chemiluminescence system. Because the reaction of luminol with hydrogen peroxide in alkaline solution in the absence of a catalyst, is relatively slow, leading to relatively weak CL intensity. Therefore, it is assumed that the enhanced CL by catalyst nanoparticles may be ascribed to their interaction with the reactants or the intermediates of the reaction of luminol with hydrogen peroxide. CuO nanoparticles due to their surface properties (large surface area) could absorb CL reactants, as a result, their reactivity and CL intensity at the time increased. Recently, it was proposed that CuO nanoparticles could efficiently catalyze the H_2O_2 decomposition the decomposition and the formation of some reactive intermediates such as hydroxyl radical ($OH^{\bullet}$), superoxide anion radical ($O^{2\bullet-}$) [38, 41]. So, in the

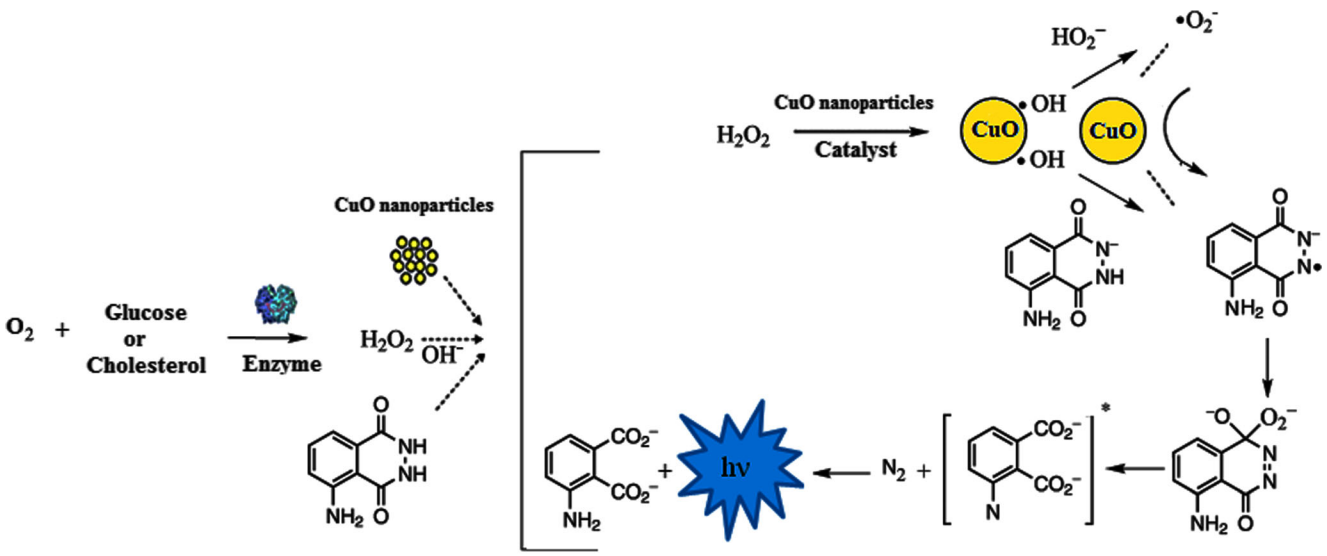

Scheme 1 The possible mechanism for the luminol- CuO nanoparticles-H_2O_2 system

luminol- CuO NPs- H_2O_2 system, the enhancement of the CL intensity can be attributed to the formation of superoxide anion radical, which further reacted with luminol anion radical under electron-transfer processes on the surface of CuO nanoparticles to produce the key intermediate (the excited-state 3-aminophthalate anion) that is a light emitter at 425 nm. Scheme 1 shows the possible CL mechanism of the luminol-CuO NPs- H_2O_2 system.

Conclusion

In summary, in this study we have found that cupric oxide nanoparticles could enhance the luminol-H_2O_2 CL signals greatly up to 28 folds. The enhancement of CL was suggested to attribute to the peroxidase-like activity of CuO nanoparticles as a nanocatalyst, which effectively catalyzed the decomposition of hydrogen peroxide into hydroxyl and superoxide radicals. The proposed CL system under the optimal conditions has good linearity, high sensitivity and precision and the method has been successfully applied to the determination glucose and cholesterol in biologic sample at pH 7. Compared with the previous methods [41–55], the proposed method provided a good limit of detection and a relatively wide linear working range. Therefore, when the luminol nanocatalytic oxidation reaction by CuO NPs was coupled with the catalytic oxidation reaction by enzyme, a simple, low-cost and very sensitive CL glucose and cholesterol biosensing system was constructed.

Compliance with Ethical Standards This work is a part of the Ph.D thesis of Miss Mahjoobeh Ehsani. The work was down in the analytical labs of Chemistry Department in University of Mazandaran. The manuscript has not been submitted to any other journals. Also the manuscript has not been published previously (partly or in full).

References

1. Fereja TH, Hymete A, Gunasekaran T (2013) A recent review on chemiluminescence reaction, principle and application on pharmaceutical analysis. Int Sch Res Notes 2013:1–12
2. Han J, Jose J, Mei E, Burgess K (2007) Chemiluminescent energy-transfer cassettes based on luorescein and nile red. Angew Chem Int Ed 46:1684–1687
3. Aboul-Enein HY, Stefan RI, van Staden JF, Zhang XR, Garcia CAM (2000) Recent developments and applications of chemiluminescence sensors. Rev Anal Chem 30:271–289
4. Kiba N, Miwa T, Tachibana M, Tani K, Koizumi H (2002) Chemiluminometric sensor for simultaneous determination of L-glutamate and L-lysine with immobilized oxidases in a flow injection system. Anal Chem 74:1269–1274
5. Tsogas GZ, Giokas DL, Vlessidis AG, Evmiridis NP (2006) Sensitivity enhancement of liquid chromatographic-direct chemiluminescence detection by on-line post-column solvent mediated preoxidative chemiluminescence. J Chromatogr A 1107:208–215
6. Tsogas GZ, Giokas DL, Vlessidis AG, Evmiridis NP (2006) The effects of solvent preoxidation on inhibited chemiluminescence of pyrogallol oxidation in flow injection analysis and liquid chromatography. Anal Chim Acta 565:56–62
7. Giokas DL, Vlessidis AG, Evmiridis NP (2007) Chemical analysis through CL-detection assisted by periodate oxidation. Anal Chim Acta 589:59–69
8. Albrecht HO (1928) "Über die Chemiluminescenz des Aminophthalsäurehydrazids" (On the chemiluminescence of aminophthalic acid hydrazide) Z. Phys Chem 136:321–330
9. Rodrı'guez-Lopez JN, Lowe DJ, Herna'ndez-Ruiz J, Hiner ANP, Garcı'a-Canovas F, Thorneley RNF (2001) Mechanism of reaction of hydrogen peroxide with horseradish peroxidase: Identification of intermediates in the catalytic cycle. J Am Chem Soc 123:11838–11847
10. Kricka LJ (2003) Clinical applications of chemiluminescence. Anal Chim Acta 500:279–286
11. Badocco D, Pastore P, Favaro G, Macca C (2007) Effect of eluent composition and pH and chemiluminescent reagent pH onion chromatographic selectivity and luminol-based chemiluminescence detection of Co^{2+}, Mn^{2+} and Fe^{2+} at trace levels. Talanta 72:249–255
12. Giokas, Vlessidis AG, Tsogas GZ, Evmiridis NP (2010) Nanoparticle-assisted chemiluminescence and its applications in analytical chemistry Dimosthenis. Trends Anal Chem 29:1113–1126
13. Dubas ST, Pimpan V (2008) Green synthesis of silver nanoparticles for ammonia sensing. Talanta 76:29–33
14. Kapakoglou NI, Giokas DL, Tsogas GZ, Lantavos AK, Vlessidis AG (2009) Development of a chromium speciation probe based on morphology-dependent aggregation of polymerized vesicle-functionalized gold nanoparticles. Analyst 134:2475–2483
15. Koutsoulis NP, Giokas DL, Tsogas GZ, Vlessidis AG (2010) Alkaline earth metal effect on the size and color transition of citrate-capped gold nanoparticles and analytical implications in periodate-luminol chemiluminescence. Anal Chim Acta 669:45–52
16. Cava RJ (1990) Structural chemistry and the local charge picture of copper oxide superconductors. Science 247:656–662
17. Tranquada JM, Sternlieb BJ, Axe JD, Nakamura Y, Uchida S (1995) Evidence for stripe correlations of spins and holes in copper oxide superconductors. Nature 375:561–565
18. Kwak K, Kim C (2005) Viscosity and thermal conductivity of copper oxide nanofluid dispersed in ethylene glycol, Korea–Aust. Rheol J 17:35–40
19. Toghill KE, Compton RG (2010) Electrochemical non-enzymatic glucose sensors: a perspective and an evaluation. Int J Electrochem Sci 5:1246–1301
20. Zhao S, Zhang K, Bai Y, Yang W, Sun C (2006) Glucose oxidase/colloidal gold nanoparticles immobilized in Nafion film on glassy carbon electrode: Direct electron transfer and electrocatalysis. Bioelectrochem 69:158–163
21. Cao X, Sun Y, Ye Y, Li Y, Ge X (2014) Macroporous ordered silica foam for glucose oxidase immobilisation and direct electrochemical biosensing. Anal Methods 6:1448–1454
22. Wojnicki M, Luty-Błocho M, Dobosz I, Grzonka J, Pacławski K, Kurzydłowski K, Fitzner K (2013) Electro-oxidation of glucose in alkaline media on graphene sheets decorated with gold nanoparticles. Mater Sci Appl 4:162–169
23. Andrade I, Santos L, Ramos F (2013) Advances in analytical methods to study cholesterol metabolism: the determination of serum noncholesterol sterols. Biomed Chromatogr 27:1234–1242
24. Karimi S, Ghourchian H, Rahimi P, Al H (2012) Rafiee-Pour, a nanocomposite based biosensor for cholesterol determination. Anal Methods 4:3225–3231
25. Panza F, Capurso C, D'Introno A, Colacicco AM, Vasquez F, Pistoia G, Capurso A, Solfrizzi V (2006) Serum total cholesterol as a biomarker for Alzheimer's disease: mid-life or late-life determinations? Exp Gerontol 4:805–806

26. Brown HH, Zlatkis A, Zak B, Boyle AJ (1954) Rapid procedure for determination of free serum cholesterol. Anal Chem 26:397–399
27. Matsubara C, Kudo K, Kawashita T, Takamura K (1985) Spectrophotometric determination of hydrogen peroxide with titanium 2-((bromopyridyl)azo)-5-(*N*-propyl-*N*-sulfopropylamino)-phenol reagent and its application to the determination of serum glucose using glucose oxidase. Anal Chem 57:1107–1109
28. Economou A, Panoutsou P, Themelis DG (2006) Enzymatic chemiluminescent assay of glucose by sequential-injection analysis with soluble enzyme and on-line sample dilution. Anal Chim Acta 572: 140–147
29. Lepore M, Portaccio M, De Tommasi E, De Luca P, Bencivenga U, Maiuri P, Mita DG (2004) Glucose concentration determination by means of fluorescence emission spectra of soluble and insoluble glucose oxidase: some useful indications for optical fibre-based sensors. J Mol Catal B: Enzym 31:151–158
30. Fromm H, Amin P, Klein H, Kupke I (1980) Use of a simple enzymatic assay for cholesterol analysis in human bile. J Lipid Res 21: 259–261
31. Montgomery DC (1997) Design and analysis of experiments, 4th edn. Wiley, New York
32. Evans M (ed) (2003) Optimization of manufacturing processes: a response surface approach. Carlton House Terrace, London
33. Zhu J, Li D, Chen H, Yang X, Lu L, Wang X (2004) Highly dispersed CuO nanoparticles prepared by a novel quick-precipitation method. Mater Lett 58:3324–3327
34. Klong HP, Alexander LF (1954) X-Ray difraction procedures for crystalline and amorphous materials. Wiley, New York
35. Box G, Behnken DW (1960) Some new three level designs for the study of quantitative variables. Technometrics 2:455–475
36. Adinarayana K, Ellaiah P (2002) Response surface optimization of the critical medium components for the production of alkaline protease by a newly isolated Bacillus sp. J Pharm Pharm Sci 5:272–278
37. Yu WW, Qu L, Guo W, Peng X (2003) Experimental determination of the extinction coefficient of CdTe, CdSe, and CdS nanocrystals. Chem Mater 15:2854–2860
38. Guo J, Cui H, Zhou W, Wang W (2008) Ag nanoparticle-catalyzed chemiluminescence reaction between luminol and hydrogen peroxide. J Photochem Photobiol A 193:89–96
39. Lind J, Merenyi G, Eriksen TE (1983) Chemiluminescence mechanism of cyclic hydrazides such as luminol in aqueous solutions. J Am Chem Soc 105:7655–7661
40. Merényi G, Lind J, Eriksen TE (1990) Luminol chemiluminescence. Chem Excitation Emitter 5:53–56
41. Oliveira Brett AMCF, Gil MH, Piedade AP (1992) An electrochemical bienzyme membrane sensor for free cholesterol. Bioelectrochem Bioenerg 28:105–115
42. Jinghua Y, Ge L, Dai P, Ge S (2010) Shiquan Liu a novel enzyme biosensor for glucose based on rhodanine derivative chemiluminescence system and mesoporous hollow silica microspheres receptor. Biosens Bioelectron 25:2065–2070
43. Zargoosha K, Chaichi MJ, Shamsipur M, Hossienkhani S, Asgharib S, Qandaleee M (2012) Highly sensitive glucose biosensor based on the effective immobilization of glucose oxidase/carbon-nanotube and gold nanoparticle in nafion film and peroxyoxalate chemiluminescence reaction of a new fluorophore. Talanta 93:37–43
44. Çubuk S, Kök Yetimoğlu E, Kahraman MV, Demirbilek P, Firlak M (2013) Development of photopolymerized fluorescence sensor for glucose analysis. Sens Actuators B Chem 181:187–193
45. Sing H, Su H, Cheng P, Chen Y (2013) Electrochemical oxidation and determination of glucose using cyclic voltammetry and a one-step prepared nanoporous gold wire electrode. J Chin Chem Soc 60: 1380–1386
46. Debruyne D, Deschaume O, Trekker J, Van Bael MJ, Bartic C (2012) Enzyme conjugation and biosensing with quantum dots: a photoluminescence study. Nanotechnology 12:1–4
47. Lan D, Li B, Zhang Z (2008) Chemiluminescence flow biosensor for glucose based on gold nanoparticle-enhanced activities of glucose oxidase and horseradish peroxidase. Biosens Bioelectron 24: 934–938
48. Lim KR, Park JM, Choi HN, Yo W (2013) Lee, gold glyconanoparticle-based colorimetric bioassay for the determination of glucose in human serum. Microchem J 106:154–159
49. Wang Y, He Q, Dong Y, Chen H (2010) In-channel modification of biosensor electrodes integrated on a polycarbonate microfluidic chip for micro flow-injection amperometric determination of glucose Sens. Actuators B Chem 145:553–560
50. Norouzi P, Faridbod F, Nasli-Esfahani E, Larijani B, Ganjali MR (2010) Biosensor based on MWCNTs-MnO2 nanoparticles using FFT continuous cyclic voltammetry. Int J Electrochem Sci 5:1008–1017
51. Chatterjee A, Majumdar S (2014) An amperometric approach towards construction of a cholesterol biosensor. Int J Adv Res 2:53–758
52. Bongiovanni C, Ferri T, Poscia A, Varalli M, Santucci R, Desideri A (2001) An electrochemical multienzymatic biosensor for determination of cholesterol. Bioelectrochem 54:17–22
53. Li Z, Jia-Jia T, Guo-Bing X, Chao G (2012) Determination of cholesterol in milk by HPLC. Food Sci 33:216–218
54. Wisitsoraat A, Karuwan C, Wong-ek K, Phokharatkul D, Sritongkham P, Tuantranont A (2009) High sensitivity electrochemical cholesterol sensor utilizing a vertically aligned carbon nanotube electrode with electropolymerized enzyme immobilization. Sensors 9:8658–8668
55. Zhang M, Yuan R, Chai Y, Chen S, Zhong H, Wang C, Cheng Y, Zhang M (2012) A biosensor for cholesterol based on gold nanoparticles-catalyzed luminol electrogenerated chemiluminescence. Biosens Bioelectron 32:288–292